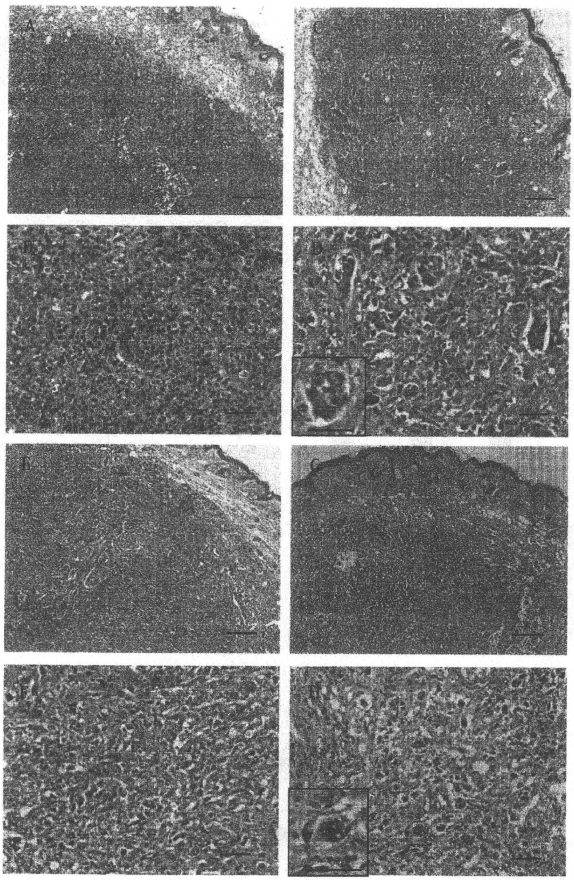

Figure 3. The histological findings of BNCT-treated SAS/mp53 tumours. Nude mice carrying SAS/mp53 tumours were treated as described in Figure 1 and sacrificed at 6 (C, D), 12 (E, F),and 48 (G, H) h after BNCT and the tumours were subjected to histological examination. Tumours in untreated control animals were also examined (A, B). Bars, 200 $\mu$m in A, C, E and G, and 50 $\mu$m in B, D, F and H.

were observed in tumours with wild-type p53. To clarify the difference between SAS/neo and SAS/mp53 tumours, only large cells with more than six nuclei were counted. It reached a peak at 6 h after BNCT and declined thereafter. In SAS/neo tumours, cells showed heterogeneity, but such multinucleated giant cells were rarely observed (Figure 4).

*The expression and/or phosphorylation of checkpoint-related proteins by BNCT*

Proteins were prepared from BNCT-treated tumours and subjected to an immunoblot analysis. In SAS/neo cells, the expression and phosphorylation of p53 increased from 12 h after BNCT and levels were maintained until 48 h (Figure 5). The phosphorylation of Rb, essential to initiate DNA synthesis, was

maintained at low levels. In SAS/mp53 tumours, the protein level of p53 was not specifically altered by BNCT, but the phosphorylation was decreased from 12 h. The phosphorylation of Rb was markedly decreased from 6 h after BNCT and became undetectable at 24 h, indicating the suppression of DNA synthesis (Figure 5).

In SAS/neo tumours, the expression of Wee1 and cyclin B1 increased at 12 h after BNCT and cdc2 was phosphorylated at 48 h (Figure 6), indicating G2 arrest long after BNCT. In SAS/mp53 tumours, phosphorylated Wee1, cyclin B1 and cdc2 were detected at high levels as compared with levels in SAS/neo tumours. At 6 h after BNCT, Wee1 and cyclin B1 levels were not altered, but the level of phosphorylated cdc2 was markedly decreased (Figure 6). The expression of Wee1 and cyclin B1 was maintained from 12 h at low levels. A temporary increase in phosphorylated cdc2 but not cdc2 protein was observed at 24 h after BNCT, indicating cell cycle arrest at the G2 checkpoint.

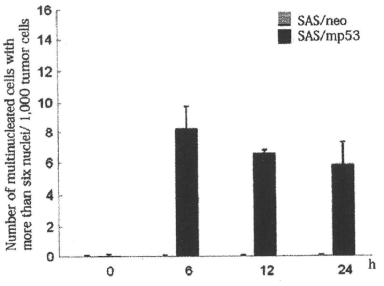


Figure 4. Multinucleated giant cells in BNCT-treated tumours. Tumour-bearing mice were treated with BNCT as described in Figure 1. The tumours were subjected to histological examination at 6 h, 12, 24, and 48 h after BNCT. Multinucleated giant cells with more than 6 nuclei were counted in each section and the number of multinucleated giant cells per 1,000 tumour cells was determined. Data are means ± SD of three determinations.

## Discussion

Critical to the application of BNCT to malignant tumours is the accumulation of $^{10}B$ into the tumour tissues as compared with the surrounding normal tissues. We used two mutated oral SCC cell lines, SAS/neo and SAS/mp53, with the same background. Two hours after the injection of BPA at a dose of 250 mg/kg body weight, $^{10}B$ concentrations in skin were 4.35 and 4.59 ppm, whereas those in the SAS/neo and SAS/mp53 tumours increased to as much as 16.56 and 17.30 ppm, respectively. The $^{10}B$ concentrations in nude mouse tumours were much higher those in skin. It seems that the tumours, irrespective of p53 status, were destroyed by BNCT selectively.

BNCT significantly suppressed the growth of tumours. SAS/neo tumours with wild-type p53

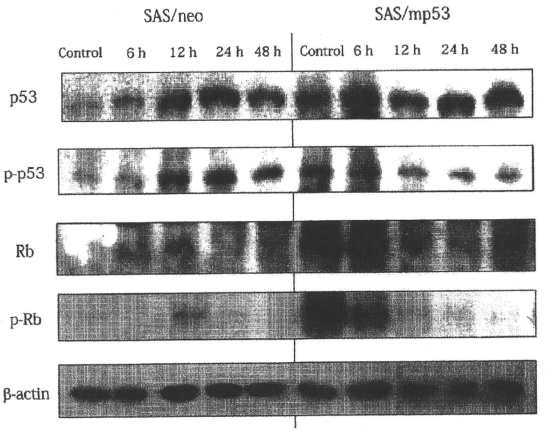


Figure 5. Immunoblot analysis of the expression and/or phosphorylation of G1 checkpoint-related proteins. SAS/neo and SAS/mp53 tumours were treated with BNCT, and the expression of p53 and Rb, and their phosphorylation were examined at 6, 12, 24, and 48 h after BNCT.

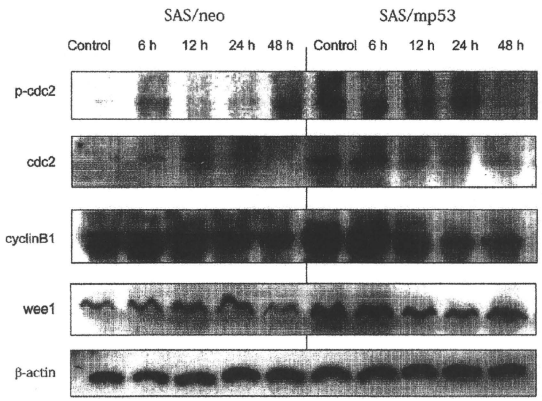


Figure 6. Immunoblot analysis of the expression and/or phosphorylation of G2 checkpoint-related proteins. SAS/neo and SAS/mp53 tumours were treated with BNCT, and the expression of cdc2, cyclin B1 and Wee1, and the phosphorylation of cdc2 were examined at 6, 12, 24, and 48 h after BNCT.

became undetectable and no recurrence occurred during the experimental period. It is hypothesised that cells resistant to BPA-mediated BNCT are basically non-proliferating cells in tumours, because BPA is selectively incorporated into proliferating cells (Ono et al. 1996, Pignol et al. 1998). There must be non-proliferating cells in SAS/neo tumours. However, our results indicate that SAS/neo tumours with wild-type p53 can be eradicated by BNCT at a dose of 13 Gy. In contrast, SAS/mp53 tumours with mutant-type p53 recurred after an interval of 2 months. Some SAS/mp53 tumour cells must survive the therapy, even when treated with BNCT at a similar dose to SAS/neo tumours. It was suspected that SAS/mp53 tumour had an advantage over SAS/neo tumour with wild-type p53 in the growth on nude mouse (Figure 1). However, even if the treated tumours were observed for more than 11 weeks, recurrence of SAS/neo tumours did not occur. Thus, the resistance of SAS/mp53 tumours to the BPA-mediated BNCT can be ascribed to the p53 mutation, but not the growth potential of tumours. Previously, we reported that neutron beam alone partly inhibited the growth of SAS tumours with wild-type p53, although BPA-mediated BNCT suppressed the tumours completely (Kamida et al. 2006). Whether neutron beam alone could affect the growth of SAS/neo and SAS/mp53 tumours in a similar manner remains to be clarified.

Kreimann et al. (2001) identified vacuolation as one of the morphological changes after BPA-mediated BNCT in hamster buccal pouch tumours. Aromando et al. (2009) indicated that BNCT had a marked inhibitory effect on DNA synthesis in hamster cheek pouch tumours and that apoptosis did not have a significant role in BNCT-induced tumour control. We found morphological changes such as chromosomal condensation, micronucleation, nuclear segmentation and vacuolation throughout the BNCT-treated SAS/neo and SAS/mp53 tumours. This means extensive cytoplasmic loss and nuclear damage by BNCT in a large number of tumour cells, followed by necrosis and/or apoptosis. However, our most striking finding was the appearance of multinucleated giant cells in SAS/mp53 tumours. Mitotic catastrophe has been widely described in tumours with mutant-type p53 after treatment with radiation and chemotherapeutic agents. Our results indicate that a morphological alteration resembling to mitotic catastrophe occur by BNCT in vivo.

The mitotic cycle is dependent upon the actions of the mitosis-promoting factor, which is a complex comprising cyclin B1 and cdc2 kinase. The constitutive activation of cyclin B1-associated cdc2 kinase overrides p53-mediated G2-M arrest and inactivation of cdc2 kinase through cdc2 and cyclin B1 repression is an essential step in p53-mediated G2-M arrest (Park et al. 2000). Wee1 protein kinase renders cdc2 inactive through phosphorylation at tyrosine-15 and threonine-14, but Cdc25 activates the cdc2/cyclin B1 complex by dephosphorylating these residues (Parker et al. 1991). In SAS/neo tumours, there was an increase in the expression of

Wee1 and cyclin B1 until 12 h and increase in phosphorylated cdc2 at 48 h after BNCT. Thus, the cell cycle of SAS/neo tumours seems to be arrested at G2 in response to BNCT. This result is consistent with our previous findings indicating that SAS and SAS/neo cells were arrested at the G2 checkpoint after BNCT in culture (Kamida et al. 2008, Fujita et al. 2009). In untreated SAS/mp53 tumours, the expression of Wee1, cyclin B1 and phosphorylation of cdc2 were maintained at high levels. The most striking change caused by BNCT was the rapid reduction of cdc2 phosphorylation at 6 h when mitotic catastrophe occurred remarkably (Figure 6). In this regard, Jin et al. (1998) reported that ectopic overexpression of cyclin B1 plus cdc2 can result in premature chromatin condensation and mitotic catastrophe. Since cyclin B1 levels in SAS/mp53 tumours were maintained at 6 h after BNCT, cyclin B1 and dephosphorylated cdc2 would form the complex, which allowed cells in the G2 phase to commit premature mitosis and multinucleation.

It was reported that polygenomic cells produced after damage of genomic DNA arise from G2 arrested cells by a series of restitution cycles by polyploidising mitoses (Nagl 1990, Hall et al. 1996). In the present study, the phosphorylation of Rb, required for DNA synthesis, was markedly reduced after BNCT (Figure 5). Since the number of multinucleated giant cells reached a maximal level at 6 h and then decreased gradually, it is unlikely that restitution plays a major role in the early formation of multinucleated giant cells. However, it has been also shown that cells escape the checkpoint without completion of cell division and become tetraploid (Brito and Rieder 2006). Mitotic cells appeared in the BNCT-treated tumours would play a role in the formation of multinucleated giant cells. The mechanism by which multinucleated giant cells are produced in the tumours with mutant-type of p53 can be considered as follows: Rapid cytolysis occurs in BNCT-sensitive cells at first, and surviving mitotic and interphase cells form cell clusters. As the next step, mitotic cells promote cell fusion in the clusters, resulting in multinucleated giant cells (Figure 3D) that are different from those produced by several polyploidising mitoses. Thereafter, the nuclei of multinucleated giant cells pycnotise and cells are going to die (Figure 3E). In the case of SAS/neo, most cells die by apoptosis or necrosis through G1 and G2 arrests, and premature mitosis is prevented. Further study is required to analyse the morphological alterations that occur in tumours with mutant-type of p53.

There is no broad consensus on the use of mitotic catastrophe, and the Nomenclature Committee on Cell Death recommends the use of expressions such as cell death preceded by multinucleation or cell death occurring during metaphase (Kroemer et al. 2009). Vakifahmetoglu et al. (2008) stated that mitotic catastrophe represents a prestage of apoptosis or necrosis. Nevertheless, there are several examples that permit mitotic catastrophe to be a cell survival mechanism. After mitotic catastrophe, a small proportion of endopolyploid tumour cells may be viable, segregate successfully and return to mitosis (Erenpreisa and Cragg 2001, Prieur-Carrillo et al. 2003). Although multinucleation observed in BNCT-treated tumours with mutant-type of p53 was similar, but not identical to mitotic catastrophe reported in vitro (Eriksson et al 2007, Maalouf et al. 2009), it may also contribute to the survival of oral SCC cells. A few cells can survive BNCT by other mechanism provided by non-functional p53, which is displayed later.

In conclusion, we demonstrated an early induction of multinucleation in BNCT-treated oral SCC tissues. BNCT is effective for advanced cancer, but recurrence occurs (Zonta et al. 2009). Approximately 50% of SCC have a mutational change of p53 (Hainaut et al. 1997). A return to the mitotic cycle of the treated cells should be blocked to ensure the long-term effect of BNCT for oral SCC with mutant-type p53.

**Declaration of interest:** This work was supported in part by a Grant-in-Aid (21390536) for Scientific Research from the Ministry of Education, Science and Culture of Japan. The authors report no conflicts of interest. The authors alone are responsible for the content and writing of the paper.

## References

Aromando RF, Heber EM, Trivillin VA, Nigg DW, Schwint AE, Itoiz ME. 2009. Insight into the mechanisms underlying tumour response to boron neutron capture therapy in the hamster cheek pouch oral cancer model. Journal of Oral Pathology and Medicine 38:448–454.

Barth RF, Coderre JA, Vicente MG, Blue TE. 2005. Boron neutron capture therapy of cancer: Current status and future prospects. Clinical Cancer Research 11:3987–4002.

Brito DA, Rieder CL. 2006. Mitotic checkpoint slippage in humans occurs via cyclin B destruction in the presence of an active checkpoint. Current Biology 16:1194–1200.

Coderre JA, Button TM, Micca PL, Fisher CD, Nawrocky MM, Liu HB. 1994. Neutron capture therapy of the 9L rat gliosarcoma using the p-boronophenylalanine-fructose complex. International Journal of Radiation Oncology, Biology, Physics 30:643–652.

Coderre JA, Morris GM. 1999. The radiation biology of boron neutron capture therapy. Radiation Research 151:1–18.

Debatin KM, Krammer PH. 2004. Death receptors in chemotherapy and cancer. Oncogene 23:2950–2966.

Erenpreisa J, Cragg MS. 2001. Mitotic death: A mechanism of survival? A review. Cancer Cell International 1:1.

Eriksson D, Löfroth PO, Johansson L, Riklund KA, Stigbrand T. 2007. Cell cycle disturbances and mitotic catastrophes in HeLa Hep2 cells following 2.5 to 10 Gy of ionizing radiation. Clinical Cancer Research 13:5501s–5508s.

Fujita Y, Kato I, Iwai S, Ono K, Suzuki M, Yoshinori Sakurai, Ken Ohnishi, Takeo Ohnishi and Yoshiaki Yura. 2009. Role of p53 mutation in the effect of boron neutron capture therapy on oral squamous cell carcinoma. Radiation Oncology 4:63.

Fukuda H, Hiratsuka J, Kobayashi T, Sakurai Y, Yoshino K, Karashima H, Turu K, Araki K, Mishima Y, Ichihashi M. 2003. Boron neutron capture therapy (BNCT) for malignant melanoma with special reference to absorbed doses to the normal skin and tumor. Australasian Physical and Engineering Sciences in Medicine 26:97–103.

Hainaut P, Soussi T, Shomer B, Hollstein M, Greenblatt M, Hovig E, Harris CC, Montesano R. 1997. Database of p53 gene somatic mutations in human tumors and cell lines: Updated compilation and future prospects. Nucleic Acids Research 25:151–157.

Hall LL, Th'ng JP, Guo XW, Teplitz RL, Bradbury EM. 1996. A brief staurosporine treatment of mitotic cells triggers premature exit from mitosis and polyploid cell formation. Cancer Research 56:3551–3559.

Ianzini F, Bertoldo A, Kosmacek EA, Phillips SL, Mackey MA. 2006. Lack of p53 function promotes radiation-induced mitotic catastrophe in mouse embryonic fibroblast cells. Cancer Cell International 6:11.

Jin P, Hardy S, Morgan DO. 1998. Nuclear localization of cyclin B1 controls mitotic entry after DNA damage. Journal of Cell Biology 141:875–885.

Kamida A, Obayashi S, Kato I, Ono K, Suzuki M, Nagata K, Sakurai Y, Yura Y. 2006. Effects of boron neutron capture therapy on human oral squamous cell carcinoma in a nude mouse model. International Journal of Radiation Biology 82:21–29.

Kamida A, Fujita Y, Kato I, Iwai S, Ono K, Suzuki M, Sakurai Y, Yura Y. 2008. Effect of neutron capture therapy on the cell cycle of human squamous cell carcinoma cells. International Journal of Radiation Biology 84:191–199.

Kankaanranta L, Seppälä T, Koivunoro H, Saarilahti K, Atula T, Collan J, Salli E, Kortesniemi M, Uusi-Simola J, Mäkitie A, Seppänen M, Minn H, Kotiluoto P, Auterinen I, Savolainen S, Kouri M, Joensuu H. 2007. Boron neutron capture therapy in the treatment of locally recurred head and neck cancer. International Journal of Radiation Oncology, Biology, Physics 69:475–482.

Kato I, Ono K, Sakurai Y, Ohmae M, Maruhashi A, Imahori Y, Kirihata M, Nakazawa M, Yura Y. 2004. Effectiveness of BNCT for recurrent head and neck malignancies. Applied Radiation and Isotopes 2061:1069–1073.

Kreimann EL, Itoiz ME, Longhino J, Blaumann H, Calzetta O, Schwint AE. 2001. Boron neutron capture therapy for the treatment of oral cancer in the hamster cheek pouch model. Cancer Research 61:8638–8642.

Kroemer G, Galluzzi L, Vandenabeele P, Abrams J, Alnemri ES, Baehrecke EH, Blagosklonny MV, El-Deiry WS, Golstein P, Green DR, Hengartner M, Knight RA, Kumar S, Lipton SA, Malorni W, Nuñez G, Peter ME, Tschopp J, Yuan J, Piacentini M, Zhivotovsky B, Melino G; Nomenclature Committee on Cell Death 2009. 2009. Classification of cell death: Recommendations of the Nomenclature Committee on Cell Death. Cell Death and Differentiation 16:3–11.

Maalouf M, Alphonse G, Colliaux A, Beuve M, Trajkovic-Bodennec S, Battiston-Montagne P, Testard I, Chapet O, Bajard M, Taucher-Scholz G, Fournier C, Rodriguez-Lafrasse C. 2009. Different mechanisms of cell death in radiosensitive and radioresistant p53 mutated head and neck squamous cell carcinoma cell lines exposed to carbon ions and x-rays. International Journal of Radiation Oncology, Biology, Physics 74:200–209.

Masunaga S, Ono K, Takahashi A, Sakurai Y, Ohnishi K, Kobayashi T, Kinashi Y, Takagaki M, Ohnishi T. 2002. Impact of the p53 status of the tumor cells on the effect of reactor neutron beam irradiation, with emphasis on the response of intratumor quiescent cells. Japanese Journal of Cancer Research 93:1366–1377.

Miyatake S, Kawabata S, Yokoyama K, Kuroiwa T, Michiue H, Sakurai Y, Kumada H, Suzuki M, Maruhashi A, Kirihata M, Ono K. 2009. Survival benefit of Boron neutron capture therapy for recurrent malignant gliomas. Journal of Neuro-Oncology 91:199–206.

Nagl W. 1990. Polyploidy in differentiation and evolution. International Journal of Cell Cloning 8:216–223.

Obayashi S, Kato I, Ono K, Masunaga S, Suzuki M, Nagata K, Sakurai Y, Yura Y. 2004. Delivery of $^{10}$boron to oral squamous cell carcinoma using boronophenylalanine and borocaptate sodium for boron neutron capture therapy. Oral Oncology 40:474–482.

Okada H, Mak TW. 2004. Pathways of apoptotic and non-apoptotic death in tumour cells. Nature Reviews. Cancer 4:592–603.

Ono K, Masunaga S, Kinashi Y, Takagaki M, Akaboshi M, Kobayashi T, Eng D, Akuta K. 1996. Radiobiological evidence suggesting heterogenous microdistribution of boron compounds in tumors: Its relation to quiescent cell population and tumor cure in neutron capture therapy. International Journal Radiation Oncology, Biology, Physics 34:1081–1086.

Ota I, Ohnishi K, Takahashi A, Yane K, Kanata H, Miyahara H, Ohnishi T, Hosoi H. 2000. Transfection with mutant p53 gene inhibits heat-induced apoptosis in a head and neck cell line of human squamous cell carcinoma. International Journal of Radiation Oncology, Biology, Physics 47:495–501.

Palme CE, Gullane PJ, Gilbert RW. 2004. Current treatment options in squamous cell carcinoma of the oral cavity. Surgical Oncology Clinics of North America 13:47–70.

Park M, Chae HD, Yun J, Jung M, Kim YS, Kim SH, Han MH, Shin DY. 2000. Constitutive activation of cyclin B1-associated cdc2 kinase overrides p53-mediated G2-M arrest. Cancer Research 60:542–545.

Parker LL, Atherton-Fessler S, Lee MS, Ogg S, Falk JL, Swenson KI, Piwnica-Worms H. 1991. Cyclin promotes the tyrosine phosphorylation of p34cdc2 in a wee1+ dependent manner. EMBO Journal 10:1255–1263.

Pignol JP, Oudart H, Chauvel P, Sauerwein W, Gabel D, Prevot G. 1998. Selective delivery of 10B to soft tissue sarcoma using10B-L-borophenylalanine for boron neutron capture therapy. British Journal of Radiology 71:320–323.

Prieur-Carrillo G, Chu K, Lindqvist J, Dewey WC. 2003. Computerized video time-lapse (CVTL) analysis of the fate of giant cells produced by X-irradiating EJ30 human bladder carcinoma cells. Radiation Research 159:705–712.

Vakifahmetoglu H, Olsson M, Zhivotovsky B. 2008. Death through a tragedy: Mitotic catastrophe. Cell Death and Differentiation 15:1153–1162.

Wong LY, Wei WI, Lam LK, Yuen AP. 2003. Salvage of recurrent head and neck squamous cell carcinoma after primary curative surgery. Head and Neck 25:953–959.

Zonta A, Pinelli T, Prati U, Roveda L, Ferrari C, Clerici AM, Zonta C, Mazzini G, Dionigi P, Altieri S, Bortolussi S, Bruschi P, Fossati F. 2009. Extra-corporeal liver BNCT for the treatment of diffuse metastases: What was learned and what is still to be learned. Applied Radiation and Isotopes 67(7–8 Suppl.):S67–75.

Mutation Research 695 (2010) 69–74

Contents lists available at ScienceDirect

Mutation Research/Genetic Toxicology and Environmental Mutagenesis

journal homepage: www.elsevier.com/locate/gentox
Community address: www.elsevier.com/locate/mutres

# Ascorbic acid 2-glucocide reduces micronucleus induction in distant splenic T lymphocytes following head irradiation

Yuko Kinashi*, Hiroki Tanaka, Shinichiro Masunaga, Minoru Suzuki, Genro Kashino, Liu Yong, Sentaro Takahashi, Koji Ono

*Research Reactor Institute, Kyoto University, Kumatori-cho, Sennan-gun, Osaka 590-0494, Japan*

ARTICLE INFO

*Article history:*
Received 13 April 2009
Received in revised form 2 November 2009
Accepted 6 December 2009
Available online 16 December 2009

*Keywords:*
Abscopal radiation effect
Ascorbic acid
T lymphocyte
Micronucleus

ABSTRACT

*Purpose:* Evidence from in vivo studies suggests there are enhanced radiation effects in abscopal regions after local head gamma ray irradiation. Splenocyte apoptosis and T lymphocyte micronuclei were induced at higher rates than what would be estimated given the dose at a shielded, distant position. In addition, we evaluated the radio-protective effects of ascorbic acid, acting as a radical scavenger on enhanced radiation effects in the shielded spleen following local head irradiation.

*Methods and materials:* The heads of C3H mice were exposed to γ-rays (10–20 Gy), while the other parts of the body were shielded with a 5 cm-thick lead block. The effective dose for the spleen was calculated at 1.0–2.0 Gy. Splenocytes were isolated 24 h after cranial irradiation and their apoptosis was measured with an Elisa kit (Roche). The induction of T lymphocyte micronuclei was studied using the cytokinesis-block micronucleus assay. The ascorbic acid glucoside, 2-O-alpha-D-glucopyranosyl-L-ascorbic acid (AA-2G), was orally administered to mice 1 h before whole body irradiation. The radio protective effects of AA-2G were estimated by comparing the induction of splenocyte damage (by apoptosis) and micronucleus induction.

*Results:* The splenocyte damage, as measured by the above two methods, was more excessive than what would be expected given exposure to 1.0–2.0 Gy of radiation. Our results suggest that the effects were enhanced in a distant, non-irradiated organ after localized irradiation. Plasma ascorbic acid concentrations were increased 8–10× over control. Treatment with ascorbic acid slightly protected mouse splenocytes from the induction of apoptosis by the enhanced effects of radiation in the abscopal region. However, ascorbic acid significantly inhibited micronucleus induction in splenic T lymphocytes following local head irradiation.

*Conclusions:* Our results suggest that ascorbic acid effectively scavenged radiation-induced radicals and protected against the enhanced effects of radiation in an abscopal region after local head gamma ray irradiation.



## 1. Introduction

The abscopal effects of radiation were first reported in 1969 and were defined as significant responses to radiation in tissues that are separate from the area exposed to the radiation [1,2].

The enhanced effects of radiation in shielded organs are thought to be based on the phenomena of so-called bystander effects. Their mechanism is thought to involve radiation signals that are transduced from the radiation-targeted organ to shielded organs [3,4]. Most have been observed in the low-dose range [3,5,6]. In fact, Prise et al. [6] noted that most bystander effects appear to saturate at higher dose levels, and that other factors must switch to hypersensitivity of a non-targeted response.

Abscopal effects from radiation have also been previously reported at therapeutic doses. For example, in studies with partially irradiated lungs, animals and patients were reported to have higher than expected tissue damage in unirradiated parts of the lung [7,8]. The mechanism for this hypersensitivity of non-targeted responses has not been elucidated, but inflammatory responses and reactive oxygen species, such as superoxide radicals, are involved [2,9].

We previously published that bystander effects were observed after boron neutron capture therapy (BNCT), and found that the radical scavenger ascorbate could effectively protect from distant damage [10]. Another group reported that radical scavengers were protective against radiation-induced bystander effects in an in vitro study [11]. Here, we investigated the possibility that 2-O-alpha-D-glucopyranosyl-L-ascorbic acid (AA-2G) had clinically relevant

* Corresponding author. Tel.: +81 72 451 2437; fax: +81 72 451 2627.
*E-mail address:* kinashi@rri.kyoto-u.ac.jp (Y. Kinashi).

1383-5718/$ – see front matter © 2009 Elsevier B.V. All rights reserved.
doi:10.1016/j.mrgentox.2009.12.002

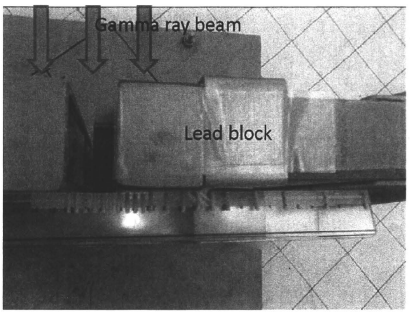


**Fig. 1.** A view from above showing the strategy for local head irradiation. The head of a mouse was irradiated while being held in a restrainer through a 2 cm slit, while the rest of its body was located behind a 5 cm lead block.

radio-protective effects. Its radio-protective effects were evaluated after induction of apoptosis in mouse splenocytes and micronuclei in splenic T cells, at a site that was distant from local head irradiation.

## 2. Materials and methods

### 2.1. Mice and ascorbic acid administration

Six-week-old female C3H/He mice were obtained from Japan Animal Inc. and acclimated to our laboratory for 8–10 weeks prior to use in experiments. AA-2G was purchased from Hayashibara Biochemical Laboratories (Okayama, Japan). C3H female mice (14–16 weeks old) were given AA-2G orally (dissolved in water, 1 mg/g of body weight), 1 h before gamma-ray irradiation. The concentration of AA-2G administration was decided after referencing previous experiments [12–14] and considering the high plasma accumulation and toxicity of ascorbic acid. Note: 1 mg of AA-2G is the equivalent of 0.52 mg of ascorbic acid. The ascorbic acid concentration in mouse plasma after AA-2G administration was measured by HPLC.

### 2.2. Irradiation

Gamma rays were delivered with a $^{60}$Co gamma-ray machine at a rate of 1.0 Gy/min. Mice were restrained in a plastic box on a radiation shelf. For partial head irradiation, heads were placed in a 2.0 cm slit in the front side of the restrainer and the rest of their bodies were shielded behind a 5 cm-thick lead block (Fig. 1). The absorbed doses for the head and the body are shown in Fig. 2. For total body irradiation (to evaluate direct splenic damage following irradiation), the whole body was irradiated (up to 5 Gy).

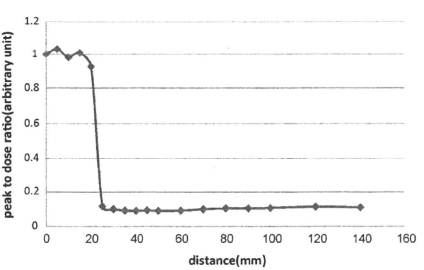


**Fig. 2.** Estimation of the amount of radiation passing through the 2 cm slit (the irradiated head dose) and into the area shielded by the lead block (the spleen dose). Each point corresponds to a red mark on the scale in Fig. 1. The intervals between the points were 5 mm (0–5 cm), 1 cm (5–10 cm) and 2 cm (10–14 cm). The head of the mouse was located in the first 2 cm (in the open region). The spleen was located at 4 cm. The dose given to the spleen was estimated at 1 Gy when 10 Gy of irradiation was given to the head.

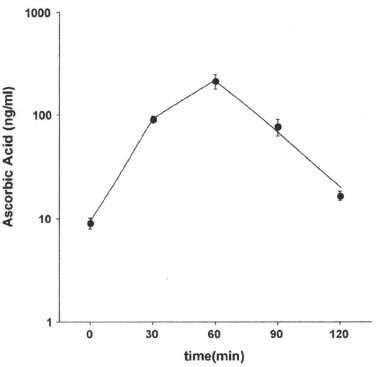


**Fig. 3.** The concentration of ascorbic acid in mouse plasma after AA-2G administration.

### 2.3. Isolation of splenocytes and splenic T lymphocytes

Details of the T lymphocyte isolation have been described elsewhere [15]. Briefly, after gamma irradiation, mice were sacrificed by cervical dislocation, and their spleens were removed, minced and washed twice in Hanks' balanced salt solution. Lymphocytes were separated using Ficoll-Hypaque gradients and were resuspended in RPMI 1640 medium (GIBCO) containing 10% fetal calf serum. The T lymphocytes were cultured at 37 °C in a humidified 5% $CO_2$ incubator. Optimum concentrations of Concanavalin A (Con A, 2 μg/mL) and 2-mercaptoethanol (2-ME, 50 μmol/mL) were used to make lymphocytes transform and divide in culture.

### 2.4. Radiation induced apoptosis and antioxidant enzyme activation

To determine splenocyte apoptosis, mice were sacrificed 24 h after irradiation and their spleens were removed. Single-cell suspensions were eliminated of erythrocytes by incubating at room temperature for 3 min in a solution of Tris-

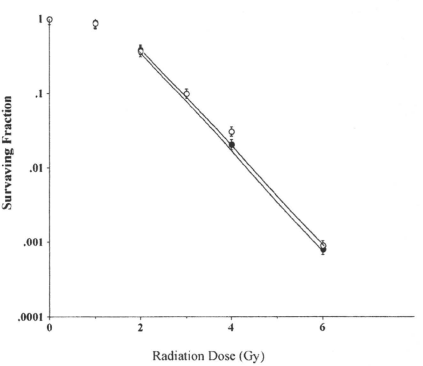


**Fig. 4.** Survival curves for splenic T lymphocytes following gamma irradiation with (open circle) or without (closed circle) ascorbic acid administration. Data represent the means ± SE of three different independent experiments. The curves for doses greater than 2 Gy were fit by linear regression analysis.

**Table 1**
Survival parameters for T lymphocytes after gamma ray irradiation with V.C. (ascorbic acid) treatment.

| Treatment | $D_0$ | $D_{10}$ |
|---|---|---|
| Gamma ray radiation | 0.65 ± 0.2 Gy | 3.0 ± 0.2 Gy |
| Gamma ray radiation with V.C. treatment | 0.85 ± 0.3 Gy | 3.1 ± 0.2 Gy |

Data pooled from three or more experiments; mean ± SE. $D_0$ and $D_{10}$ derived from survival curves following irradiation.

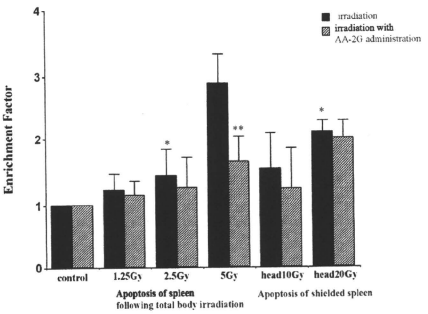


**Fig. 5.** Induction of apoptosis of mouse splenocytes after irradiation (black bars) and the effect of AA-2G administration (gray bars). Histogram bars show the means ± SE for five animals. (*) Significant increase in apoptosis compared to 2.5 Gy total body irradiation. $p < 0.05$. (**) Significant decrease in apoptosis compared to no ascorbic acid administration. $p < 0.05$.

buffered ammonium chloride. After twice washing with PBS, cells were counted and examined for induction of apoptosis. Apoptosis was detected with a sandwich immunoassay system using a cell death detection ELISA kit (Roche Diagnostic Inc.). The assay is based on the quantitative sandwich enzyme immunoassay principle, using mouse monoclonal antibodies directed against DNA and histones, respectively. Apoptosis was measured by following the ELISA protocol. The enrichment factor was the calculated absorbance of each sample divided by the absorbance of corresponding negative control. To measure the activity of catalase (CAT) and superoxide dismutase (SOD), mouse blood was obtained from the main inferior vein 60, 120 and 1200 min after irradiation. The activities of CAT and SOD in mouse plasma were detected using a colorimetric assay (SRL Research Laboratory Inc., Japan).

### 2.5. Determination of T lymphocyte survival and the micronucleus assay

Details of the assays for cell survival and micronucleus frequency have been reported previously [15]. Briefly, the survival data for lymphocytes were obtained by limiting dilution assays. To measure the cloning efficiency of lymphocytes, cells were seeded in culture medium (150 μL) at densities of 10–10,000 cells/well in 96-well tissue culture plates. The cloning efficiency was calculated from the proportion of the wells without clones, using limiting dilution analysis [16]. The cytokinesis-block micronucleus assay for lymphocytes was performed following a method described by Fenech and Morley [17] with slight modifications. Cytochalasin B (Sigma) was added to the cultured T lymphocytes at a final concentration of 5.0 μg/mL, 44 h after Con A stimulation. Eighteen hours later, cells were collected by centrifugation and resuspended in Carnoy's fixative. Next, a drop of the cell suspension was spread on a glass slide and dried, the cells were stained with Hoechst 33258 (50 μg/mL), and

**Table 3**
The micronucleus frequency per 100 binucleated T lymphocytes after irradiation and the effect of AA-2G administration.

| Total body irradiation (Gy) | | | Head irradiation 10 Gy |
|---|---|---|---|
| 0 Gy | 1.25 Gy | 2.5 Gy | |
| 2.8 ± 1.5 | 26.8 ± 6.5 | 47.9 ± 13.2 | 62.1 ± 18.5 |
| With AA-2G treatment | | | |
| 2.9 ± 1.5 | 14.9 ± 8.5** | 29.1 ± 11.5** | 24.9 ± 10.5** |

Results show the mean ± SE from at least three independent experiments.
** Significant differences were observed with AA-2G administration (Student's *t*-test; $p < 0.05$).

the frequency of micronuclei was determined on 10 separate slides by counting the total number of micronuclei per 100 binucleated cells.

### 2.6. Statistical analysis

Significance was calculated using Student's tests. Results were considered significant for values of $p < 0.05$.

## 3. Results

### 3.1. The effect of ascorbic acid treatment

The ascorbic acid concentration in mouse plasma increased and was maintained at a high level during the 30–90 min after oral administration of AA-2G. One hour after AA-2G administration (1 mg/g of mouse body weight), the concentration of ascorbic acid in the plasma was increased 4–10× over the control (Fig. 3). The plasma level of ascorbic acid increased sharply, as quickly as 30 min, and was maintained at a high level for 1.5 h after oral administration of AA-2G. The availability of AA-2G as ascorbic acid was compatible with a previous report [13].

Fig. 4 and Table 1 show survival curves and the parameters for T lymphocytes after gamma irradiation, with and without ascorbic acid treatment. These results showed that gamma radiation lethality was not affected by ascorbic acid treatment.

### 3.2. Induction of apoptosis and the activities of anti-oxidative enzymes

Apoptosis was analyzed after 1.25, 2.5 and 5 Gy of whole body irradiation and 10 and 20 Gy of local head irradiation, with and without ascorbic administration. For local head irradiation, the spleen was shielded behind a 5 cm-thick lead block (Fig. 1) and the doses of radiation absorbed by the spleen and head were measured (1.0 Gy for the spleen from 10 Gy of radiation exposure to the head; 2.0 Gy (spleen) from 20 Gy (head); Fig. 2). After 20 Gy head irradiation, the apoptosis that occurred in shielded spleen cells exceeded that which occurred when spleen cells were directly irradiated with 2.5 Gy (Fig. 5). Therefore, the damage to shielded spleen cells was more excessive than what would be expected given a dose of 2.0 Gy.

Fig. 5 also shows the induction of apoptosis in mouse splenocytes after AA-2G treatment. Ascorbic acid protected mouse

**Table 2**
SOD and catalase activity in mouse serum after treatment with AA-2G.

| Time after irradiation (min) | SOD activity (Units/mL) | | Catalase activity (Units/mL) | |
|---|---|---|---|---|
| | 6 Gy irradiation | 6 Gy irradiation with AA-2G | 6 Gy irradiation | 6 Gy irradiation with AA-2G |
| 0 | 7.7 ± 0.8 | 7.1 ± 0.7 | 1.0 ± 0.1 | 1.0 ± 0.1 |
| 60 | 9.2 ± 0.9 | 10.4 ± 1.0 | 3.6 ± 0.4 | 4.2 ± 0.4 |
| 120 | 10.0 ± 0.9 | 11.0 ± 1.0 | 3.6 ± 0.4 | 4.4 ± 0.4 |
| 1200 | 12.5 ± 1.0 | 14.0 ± 1.4 | 2.2 ± 0.2 | 4.4 ± 0.4** |

Results show the mean ± SE from at least three independent experiments.
** Significant increases were observed with AA-2G administration (Student's *t*-test; $p < 0.05$).

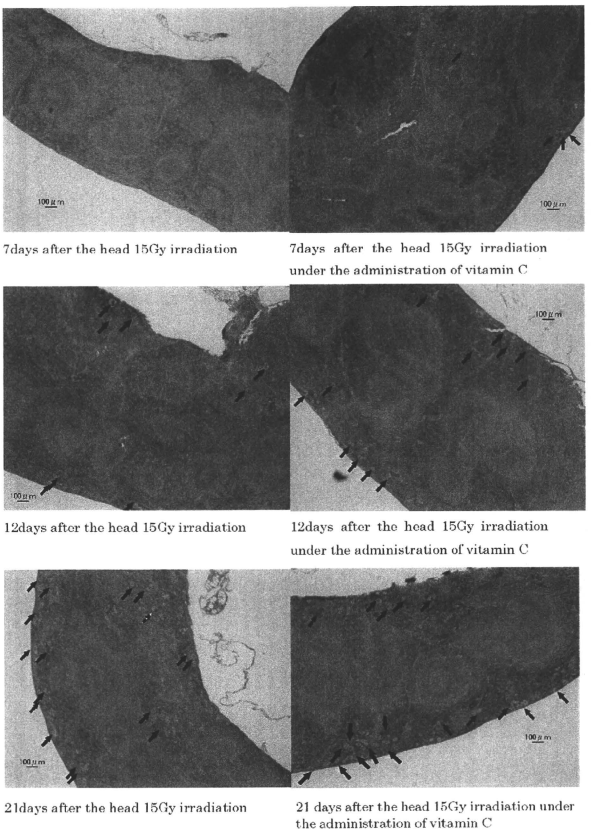


**Fig. 6.** Spleens 7–21 days after 15 Gy of head irradiation. Formalin-fixed paraffin-embedded tissue sections were HE stained. The arrows show macrophage proliferation in the spleen after the head irradiation (magnification 30×. Scale bars 100 μm).

splenocytes from apoptosis after 5 Gy whole-body irradiation. To understand how anti-oxidative enzymes participate in initial DNA damage, we investigated how treating with AA-2G affected the activation of the CAT and SOD in the plasma following a dose of 6 Gy (1 Gy in addition to the 5 Gy irradiation). AA-2G administration increased the activation of CAT and SOD slightly. A significant increase in CAT activity was observed with AA-2G treatment 20 h after irradiation (Table 2).

### 3.3. Micronucleus induction

The induction of micronuclei in mouse T lymphocytes after various treatments is shown in Table 3. Micronuclei were counted after 1.25 and 2.5 Gy of whole body irradiation and 10 Gy of local head irradiation, with and without ascorbic administration. As mentioned above, a 10 Gy dose of radiation exposure to the head corresponded to a dose of 1.0 Gy for the shielded spleen. The frequency of micronuclei induced in shielded splenic T cells with 10 Gy of head irradiation was about 2 times higher than that induced after 2.5 Gy of whole body irradiation (Table 3). Our results confirm that shielded, distant splenic T lymphocytes had more damage than what would have been anticipated, given a dose of 1.0 Gy. This again suggests that the radiation effects in a distant, shielded organ were enhanced after local irradiation. However, while treatment with ascorbic acid protected, although not significantly, against the induction of apoptosis in shielded splenocytes, ascorbic acid significantly inhibited shielded splenic T lymphocytes from forming micronuclei after local head irradiation (Fig. 5 and Table 3). Therefore, unlike its effects on induction of mouse splenocyte apoptosis, AA-2G had radioprotective

effects on the induction of T lymphocyte micronuclei after irradiation.

## 4. Discussion

In high LET therapy, as occurs in boron neutron capture therapy (BNCT) and heavy-ion radiotherapy, hypo-fractionation is acceptable and therapeutic radiation doses are larger than conventional radiotherapies. The normal tissue radiation dose for vascular endothelial cells in BNCT is estimated to be around 10–15 Gy [18]. Enhanced radiation effects in abscopal regions following large local doses of radiation have not previously been investigated. Here, we studied whether shielded splenocytes in abscopal regions suffered enhanced radiation effects after 10–20 Gy of local head gamma ray-irradiation. Splenocyte apoptosis induction and T lymphocyte micronuclei were higher than what would be expected with the estimated dose of radiation in the distant, shielded spleen.

In vivo radiation-induced bystander effects are defined as phenomena that occur when irradiation signals are transduced from an irradiated lesion to a shielded organ and induce a radiation effect in that non-irradiated, shielded organ. A previous group reported that the spleen is a target organ of local-irradiation induced bystander effects in vivo. Koturbash et al. described how cranial X-ray irradiation (1 Gy) induced DNA damage, apoptosis, and increased p53 levels in a shielded spleen [5]. They also suggested the possibility that the induction of indirect DNA damage in the shielded splenocytes was mediated by reactive oxygen species. Mechanistically, the radiation-induced bystander effect in vivo is thought to be mediated by the inflammatory response after exposure to ionizing radiation. Lorimore et al. reported that macrophage activation following a 4 Gy irradiation provided a mechanism for producing damage via bystander effects [19]. Another previous report showed that tumor cell killing by macrophages was activated with more than 10 Gy [20]. These experiments show that high dose radiation might induce bystander signaling by mediating macrophage activation. We confirmed that large dose local head irradiation (10–20 Gy) induced apoptosis and micronuclei in the distant, shielded spleen. These enhanced radiation effects in an abscopal region were induced by a large dose irradiation and may have been mediated by macrophage activation. Shown in the left column of Fig. 6, histological sections revealed macrophage proliferation in the spleen appearing on the 12th day post-irradiation and becoming severe by day 21. Macrophage proliferation in the spleen was found to be more severe after ascorbic acid administration, and to occur earlier (on the 7th day post-irradiation; shown in the right column of Fig. 6).

We evaluated the protective effects of a radical scavenger on enhanced radiation effects in the distant spleen after large doses of local head irradiation. Free radicals are one of the most important bio-chemicals that are triggered by the activation of macrophages following irradiation [21]. This suggests the possibility that radical scavengers might protect abscopal regions from enhanced radiation effects. Our study of apoptosis induction suggests that AA-2G treatment suppressed the induction of apoptosis following total body radiation. In our anti-oxidative enzyme study, AA-2G administration increased catalase activity after 20 h, which was the length of the apoptosis assay, but AA-2G did not significantly affect SOD activity. The C3H/He mouse strain is more radiation-resistant than other Balb/c mouse strains [22,23]. The different sensitivities of mouse strains to irradiation were determined by micronucleus formation in T lymphocytes and fibroblasts, and an intestinal cell survival assay [15]. A previous report demonstrated that hepatic CAT and SOD enzyme activities increased 30 min after whole body ionizing irradiation of C3H mice, suggesting that CAT and SOD may be related to the mechanism of their radiation resistance [24]. We confirmed that these antioxidant enzymes had elevated activities after irradiation and that AA-2G enhanced CAT activity. This result suggests that ascorbic acid may protect from radiation damage by inducing CAT.

We previously reported that radical scavengers are protective against neutron-induced mutations [25,26]. Furthermore, we compared the effects of DMSO (a source of short-lived radical scavengers) and ascorbic acid (a source of long-lived radical scavengers) on the induction of mutations in bystander cells. DMSO treatment slightly reduced the frequency of mutations that were induced by the bystander effect, but post-radiation ascorbic-acid treatment reduced the mutation frequency more than DMSO [10]. Recently, Harada et al. reported that ascorbic acid was an effective radical scavenger for suppressing the bystander response in vitro. They examined three types of radical scavengers, including a nitric oxide scavenger, and found that ascorbic acid was the most effective suppressor of micronucleus induction in non-irradiated bystander cells [27].

We showed that ascorbic acid significantly inhibited shielded splenic T lymphocytes from forming micronuclei following local head irradiation (Fig. 5 and Table 3). However, AA-2G did not protect shielded splenocytes against apoptosis. These results show that AA-2G treatment had radio-protective effects on T-lymphocytes in abscopal regions (in the spleen), but this did not apply to all splenic cells.

Clinically, chromosomal instability [28] and epigenetic dysregulation of DNA [29] were analyzed in non-irradiated or distant organs after irradiation. Enhanced radiation effects in abscopal regions are thought to increase the incidence of secondary, post-radiation therapy cancers. Therefore, effective radioprotection from enhanced radiation effects in abscopal regions is needed. Ascorbic acid is a well-known, important vitamin and a non-toxic radical scavenger that can be effective for protecting against enhanced radiation effects in abscopal regions during radiation therapy.

## Conflict of interest

Authors declare that there are no conflicts of interest.

## Acknowledgments

This study was supported by a Grant-in-Aid for Scientific Research from the Ministry of Education, Culture, Sports, Science and Technology of Japan.

## References

[1] M.P. Nobler, The abscopal effect in malignant lymphoma and its relationship to lymphocyte circulation, Radiology 93 (1969) 410–412.
[2] W.F. Morgan, Non-targeted and delayed effects of exposure to ionizing radiation: II. Radiation-induced genomic instability and bystander effects in vivo, clastogenic factors and transgenerational effects, Radiat. Res. 159 (2003) 581–596.
[3] K. Camphausen, M.A. Moses, C. Menard, M. Sproull, W.D. Beecken, J. Folkman, M.S. O'Reilly, Radiation abscopal antitumor effect is mediated through p53, Cancer Res. 63 (2003) 1990–1993.
[4] E.I. Azzam, J.B. Little, The radiation-induced bystander effect: evidence and significance, Hum. Exp. Toxicol. 23 (2004) 61–65.
[5] I. Koturbash, J. Loree, K. Kutanzi, C. Koganow, I. Pogribny, O. Kovalchuk, In vivo bystander effect: cranial X-irradiation leads to elevated DNA damage, altered cellular proliferation and apoptosis, and increased p53 levels in shielded spleen, Int. J. Radiat. Oncol. Biol. Phys. 70 (2007) 554–562.
[6] K.M. Prise, M. Folkard, B.D. Michael, A review of the bystander effect and its implications for low-dose exposure, Radiat. Protect. Dosimetry 104 (2003) 347–355.
[7] G.W. Morgan, S.N. Breit, Radiation and the lung: a re-evaluation of the mechanism mediating pulmpnary injury, Int. J. Radiat. Oncol. Biol. Phys. 31 (1995) 361–369.
[8] M.A. Khan, R.P. Hill, J. Van Dyk, Partial volume rat lung irradiation: an evaluation of early DNA damage, Int. J. Radiat. Oncol. Biol. Phys. 40 (1998) 467–476.

[9] K.M. Prise, M. Folkard, B.D. Michael, Bystander response induced by low LET radiation, Oncogene 22 (2003) 7043–7049.
[10] Y. Kinashi, S. Masunaga, K. Nagata, M. Suzuki, S. Takahashi, K. Ono, A bystander effect observed in boron neutron capture therapy: a study of the induction of mutations in the HPRT locus, Int. J. Radiat. Oncol. Biol. Phys. 68 (2007) 508–514.
[11] G. Kashino, K.M. Prise, K. Suzuki, N. Matsuda, S. Kodama, M. Suzuki, K. Nagata, Y. Kinashi, S. Masunaga, K. Ono, M. Watanabe, Effective suppression of bystander effects by DMSO treatment of irradiated CHO cells, J. Radiat. Res. 48 (2007) 197–204.
[12] I. Yamamoto, S. Suga, Y. Mitoh, M. Tanaka, N. Muto, Antiscorbutic activity of L-ascorbic acid 2-gluciside and its availability as a vitamin C supplement in normal rats and guinea pigs, J. Pharmacobiodyn. 13 (1990) 688–695.
[13] A. Tai, Y. Fujitani, K. Matsumoto, D. Kawasaki, I. Yamamoto, Bioability of a series of novel acylated ascorbic acid derivatives, 6-O-acyl-2-O-α-D-glucopyranosyl-L-ascorbic acids, as an ascorbic acid supplement in rats and guinea pigs, Biosci. Biotechnol. Biochem. 66 (2002) 1628–1634.
[14] L.V. d'Uscio, S. Milstien, D. Richardson, L. Smith, Z.S. Katusic, Long-term Vitamin C treatment increase vascular tetrahydrobiopterin levels and nitric oxide synthase activity, Circulat. Res. 92 (2003) 88–95.
[15] Y. Kinashi, K. Ono, M. Abe, The micronucleus assay of lymphocytes is a useful predictive assay of the radiosensitivity of normal tissue: a study of three inbred strains of mice, Radiat. Res. 148 (1997) 341–347.
[16] H. Waldmann, S. Cobbold, I. Lefkovits, Limiting dilution analysis, in: G.G.B. Klaus (Ed.), Lymphocytes, A Practical Approach, IRL, Oxford, 1987, pp. 163–188.
[17] F. Fenech, A.A. Morley, Cytokinesis-block micronucleus method in human lymphocytes: effect of in vivo aging and low dose X-irradiation, Mutat. Res. 161 (1986) 193–198.
[18] T. Kageji, S. Nagahiro, S. Uyama, Y. Mizobuchi, Y. Nakagawa, Clinical review of BNCT using mixed neutron beam in patients with malignant glioma, in: W. Sauerwein, R. Moss, A. Wittig (Eds.), Research and Development in Neutron Capture Therapy Monduzzi Editore S.p.A., Bologna, Italy, 2002, pp. 1085–1091.
[19] S.A. Lorimore, P.J. Coates, G.E. Scobie, G. Milne, E.G. Wright, Inflammatory-type responses after exposure to ionizing radiation in vivo: a mechanism for radiation-induced bystander effects? Oncogene 20 (2001) 7085–7095.
[20] L.E. Lambert, D.M. Paulnock, Modulation of macrophage function by γ-irradiation; Acquisition of the primed cell intermediate stage of macrophage tumoricidal action pathway, J. Immunol. 139 (1987) 2834–2841.
[21] G. McLennan, L.W. Oberley, A.P. Author, The role of oxygen-derived free radicals in radiation-induced damage and death of nondividing eukaryotic cells, Radiat. Res. 84 (1980) 122–132.
[22] K.H. Kohn, M.M. Kallman, The influence of strain on acute X-ray lethality in the mouse: LD50 and death rate studies, Radiat. Res. 5 (1956) 309–317.
[23] T.H. Roderic, The response of twenty-seven inbred strains of mice to daily doses of whole-body X-irradiation, Radiat. Res. 120 (1963) 631–639.
[24] R. Hardmeier, H. Hoeger, S. Fang-Kircher, A. Khoschsorur, G. Lubic, Transcription and activity of antioxidant enzymes after ionizing irradiation in radiation-resistant and radiation-sensitive mice, Proc. Natl. Acad. Sci. U.S.A. 94 (1997) 7572–7576.
[25] Y. Kinashi, Y. Sakurai, S. Masunaga, M. Suzuki, M. Akaboshi, K. Ono, Dimethyl sulfoxide protects against thermal and epithermal neutron-induced cell death and mutagenesis of Chinese hamster ovary (CHO) cells, Int. J. Radiat. Oncol. Biol. Phys. 47 (2000) 1371–1378.
[26] Y. Kinashi, Y. Sakurai, S. Masunaga, M. Suzuki, K. Nagata, K. Ono, Ascorbic acid reduced mutagenicity at the HPRT locus in CHO cells against thermal neutron radiation, Appl. Radiat. Isotopes 61 (2004) 929–932.
[27] T. Harada, G. Kashino, K. Suzuki, N. Matsuda, S. Kodama, M. Watanabe, Different involvement of radical species in irradiated and bystander cells, Int. J. Radiat. Biol. 84 (2008) 809–814.
[28] E. Gwyneth, S.A. Watson, A. Lorimore, D.A. Macdonald, E.G. Wright, Chromosomal instability in unirradiated cells induced in vivo by a bystander effect of ionizing radiation, Cancer Res. 60 (2000) 5608–5611.
[29] I. Koturbash, A. Boyko, R. Rodriguez-Juarez, R.J. MacDonald, V.P. Tryndyak, I. Kovalchuk, I.P. Pogribny, O. Kovalchuk, Role of epigenetic effects in maintenance of long-term persistent bystander effect in spleen in vivo, Carcinogenesis 28 (2007) 1831–1838.

VOLUME 28 · NUMBER 36 · DECEMBER 20 2010

JOURNAL OF CLINICAL ONCOLOGY ORIGINAL REPORT

# Phase III Trial Comparing Oral S-1 Plus Carboplatin With Paclitaxel Plus Carboplatin in Chemotherapy-Naïve Patients With Advanced Non–Small-Cell Lung Cancer: Results of a West Japan Oncology Group Study

*Isamu Okamoto, Hiroshige Yoshioka, Satoshi Morita, Masahiko Ando, Koji Takeda, Takashi Seto, Nobuyuki Yamamoto, Hideo Saka, Kazuhiro Asami, Tomonori Hirashima, Shinzoh Kudoh, Miyako Satouchi, Norihiko Ikeda, Yasuo Iwamoto, Toshiyuki Sawa, Masaki Miyazaki, Kenji Tamura, Takayasu Kurata, Masahiro Fukuoka, and Kazuhiko Nakagawa*

From the Kinki University Faculty of Medicine; Osaka City General Hospital; National Hospital Organization, Kinki-chuo Chest Medical Center; Osaka Prefectural Medical Center for Respiratory and Allergic Diseases; Osaka City University Medical School; Cancer Center, Izumi Municipal Hospital, Osaka; Kurashiki Central Hospital, Kurashiki; Yokohama City University Medical Center, Yokohama; Kyoto University School of Public Health, Kyoto; National Kyushu Cancer Center, Fukuoka; Shizuoka Cancer Center, Nagaizumi; National Hospital Organization, Nagoya Medical Center, Nagoya; Hyogo Cancer Center, Akashi; Tokyo Medical University, Tokyo; Hiroshima City Hospital, Hiroshima; Gifu Municipal Hospital, Gifu; and the Kinki University School of Medicine, Nara Hospital, Nara, Japan.

Submitted June 13, 2010; accepted September 24, 2010; published online ahead of print at www.jco.org on November 15, 2010.

Supported by Taiho Pharmaceutical Co Ltd.

Presented in part at the 46th Annual Meeting of the American Society of Clinical Oncology, Chicago, IL, June 4-8. 2010.

This study is registered with University Hospital Medical Information Network Clinical Trial Registry (http://www.umin.ac.jp/ctr/index.htm, identification number UMIN000000503).

Authors' disclosures of potential conflicts of interest and author contributions are found at the end of this article.

Clinical Trials repository link available on JCO.org.

Corresponding author: Isamu Okamoto, MD, PhD, Kinki University Faculty of Medicine, 377-2 Ohno-higashi, Osaka-Sayama, Osaka 589-8511, Japan; e-mail: chi-okamoto@dotd.med.kindai.ac.jp.



0732-183X/10/2836-5240/$20.00

DOI: 10.1200/JCO.2010.31.0326

## ABSTRACT

### Purpose

The primary goal of this open-label, multicenter, randomized phase III trial was to determine whether treatment with carboplatin plus the oral fluoropyrimidine derivative S-1 was noninferior versus that with carboplatin plus paclitaxel with regard to overall survival (OS) in chemotherapy-naive patients with advanced non–small-cell lung cancer (NSCLC).

### Patients and Methods

A total of 564 patients were randomly assigned to receive either carboplatin (area under the curve, 5) on day 1 plus oral S-1 (40 mg/m$^2$ twice per day) on days 1 to 14 or carboplatin (area under the curve, 6) plus paclitaxel (200 mg/m$^2$) on day 1 every 21 days.

### Results

At the planned interim analysis, with a total of 268 death events available, the study passed the O'Brien-Fleming boundary of 0.0080 for a positive result and noninferiority of carboplatin and S-1 compared with carboplatin and paclitaxel was confirmed for OS (hazard ratio, 0.928; 99.2% CI, 0.671 to 1.283). Median OS was 15.2 months in the carboplatin and S-1 arm and 13.3 months in the carboplatin and paclitaxel arm, with 1-year survival rates of 57.3% and 55.5%, respectively. Rates of leukopenia or neutropenia of grade 3/4, febrile neutropenia, alopecia, and neuropathy were more frequent in the carboplatin and paclitaxel arm, whereas thrombocytopenia, nausea, vomiting, and diarrhea were more common in the carboplatin and S-1 arm. The carboplatin and S-1 arm had significantly more dose delays than the carboplatin and paclitaxel arm.

### Conclusion

Oral S-1 with carboplatin was noninferior in terms of OS compared with carboplatin and paclitaxel in patients with advanced NSCLC, and is thus a valid treatment option.

*J Clin Oncol 28:5240-5246. © 2010 by American Society of Clinical Oncology*

## INTRODUCTION

Lung cancer is the leading cause of death related to cancer worldwide,[1] with non–small-cell lung cancer (NSCLC) accounting for 85% of lung cancer cases. For individuals with advanced or metastatic NSCLC, platinum-based chemotherapy is the mainstay of first-line treatment on the basis of the moderate improvement in survival and quality of life it affords compared with best supportive care alone.[2-5] Thus, there is still a need for new treatment regimens to ameliorate symptoms and prolong survival in patients with advanced NSCLC in a manner that is both convenient and safe.

S-1 (TS-1; Taiho Pharmaceutical Co Ltd, Tokyo, Japan) is an oral fluoropyrimidine agent that consists of tegafur, 5-chloro-2,4-dihydroxypyridine, and potassium oxonate in a molar ratio of 1:0.4:1.[6,7] A phase II trial of oral S-1 as a single agent for the treatment of advanced NSCLC yielded a response rate of 22% and a median survival time of 10.2 months in 59 patients without prior chemotherapy.[8] We previously performed a phase I/II study of carboplatin/S-1 combination therapy and found that administration of S-1 (40 mg/m$^2$ twice per day) on days 1 to 14 in combination with carboplatin (area under the curve [AUC], 5) on day 1 of every 3-week cycle yielded efficacy results similar to those of other platinum doublets.[9] The carboplatin and S-1 combination had a more favorable toxicity profile than that typically seen with platinum-based regimens,

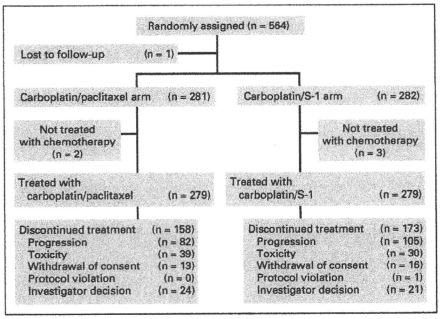


**Fig 1.** CONSORT diagram for the study.

especially with regard to neutropenia, febrile neutropenia, neuropathy, and alopecia.[9] In addition, replacement of paclitaxel with oral S-1 in combination therapy with carboplatin avoids the need for premedication to ameliorate paclitaxel-induced hypersensitivity and the 3-hour infusions required for paclitaxel administration. We therefore undertook and now report the results of the LETS (Lung Cancer Evaluation of TS-1) study, a multicenter, randomized, phase III, noninferiority trial of carboplatin and S-1 in comparison with carboplatin and paclitaxel combination therapy in chemotherapy-naive patients with advanced NSCLC.

## PATIENTS AND METHODS

### Patients

The criteria for patient eligibility included a diagnosis of NSCLC confirmed either histologically or cytologically; a clinical stage of IIIB not amenable to curative treatment or of stage IV; a measurable lesion according to the Response Evaluation Criteria in Solid Tumors (RECIST)[10]; no prior chemotherapy; an age of 20 to 74 years; an Eastern Cooperative Oncology Group (ECOG) performance status of 0 or 1; and a projected life expectancy of at least 3 months. Patients had adequate bone marrow reserve and organ function including a calculated creatinine clearance of $\geq$ 60 mL/min based on the standard Cockcroft and Gault formula. Radiation therapy for metastatic disease was permitted if it was completed at least 2 weeks before random assignment. Main exclusion criteria included active concomitant malignancy, symptomatic brain metastasis, interstitial pneumonia, watery diarrhea, heart failure, uncontrolled diabetes mellitus, active infection, and a past history of drug allergy. These inclusion and exclusion criteria are consistent with those of previous studies involving carboplatin and paclitaxel treatment.[11] Written informed consent was obtained from all patients, and the study protocol was approved by the institutional ethics committee of each of the participating institutions.

### Treatment Plan

Eligible patients were randomly assigned to receive either carboplatin (AUC, 6) plus paclitaxel (200 mg/m$^2$) on day 1[11] or carboplatin (AUC, 5) on day 1 plus oral S-1 (40 mg/m$^2$ twice per day) on days 1 to 14. Chemotherapy was repeated every 3 weeks for a maximum of six cycles unless there was earlier evidence of disease progression or intolerance of the study treatment.

### End Points

The primary objective of this open-label, multicenter, randomized phase III trial was to establish the noninferiority of S-1 plus carboplatin compared with paclitaxel plus carboplatin as first-line therapy in terms of overall survival (OS) in patients with advanced NSCLC. Secondary end points included tumor response, treatment safety, quality of life (QOL), and progression-free survival (PFS).

### Baseline and Follow-Up Assessments

Baseline evaluations included medical history, physical examination, ECG, tumor status, ECOG performance status, and laboratory analyses. During treatment, blood counts and biochemical tests were performed at least biweekly. A computed tomography scan was performed for tumor assessment within 14 days of initiation of study treatment and was repeated after every 1 to 2 months of planned therapy. All responses were defined according to RECIST. If a patient was documented as having a complete response (CR) or a

**Table 1.** Patient Demographic and Clinical Characteristics

| Characteristic | Carboplatin/Paclitaxel (n = 281) No. | Carboplatin/Paclitaxel (n = 281) % | Carboplatin/S-1 (n = 282) No. | Carboplatin/S-1 (n = 282) % | *P* |
|---|---|---|---|---|---|
| Age, years | | | | | |
| Median | 63 | | 64 | | .510 |
| Range | 36-74 | | 38-74 | | |
| Sex | | | | | |
| Male | 215 | 76.5 | 217 | 77.0 | .902 |
| Female | 66 | 23.5 | 65 | 23.0 | |
| ECOG PS | | | | | |
| 0 | 90 | 32.0 | 86 | 30.5 | .695 |
| 1 | 191 | 68.0 | 196 | 69.5 | |
| Histology | | | | | |
| Adenocarcinoma | 195 | 69.4 | 195 | 69.1 | .560 |
| Nonadenocarcinoma | 86 | 30.6 | 87 | 30.9 | |
| Clinical stage | | | | | |
| IIIB | 68 | 24.2 | 68 | 24.1 | .981 |
| IV | 213 | 75.8 | 214 | 75.9 | |
| Smoking status | | | | | |
| Smoker | 229 | 81.5 | 230 | 81.6 | .984 |
| Nonsmoker | 52 | 18.5 | 52 | 18.4 | |

Abbreviation: ECOG PS, Eastern Cooperative Oncology Group performance status.

partial response (PR), a confirmatory evaluation was performed after an interval of 4 weeks. Disease control was defined as the best tumor response among CR, PR, or stable disease that was confirmed and sustained for 6 weeks or longer. Patients were evaluated for adverse events during therapy and until 42 days after administration of the last dose of the study treatment. Toxicity was evaluated according to the National Cancer Institute Cancer Common Toxicity Criteria, version 3. QOL was assessed with the lung cancer subscale of the Functional Assessment of Cancer Therapy–Lung (FACT-L)[12] and the neurotoxicity subscale of the FACT/Gynecology Oncology Group-Neurotoxicity (GOG-Ntx) version 4.[13] In addition, alopecia was evaluated on the basis of the single item "I have been bothered by hair loss," which was included in the former version of FACT-L. The maximum attainable scores on the lung cancer subscale, neurotoxicity subscale, and alopecia item were 28, 44, and 4, respectively, with which the patient was considered to be asymptomatic. Patients were asked to complete each instrument at the time of enrollment and at 6 and 9 weeks after initiation of treatment.

### Statistical Analysis

Eligible patients were randomly assigned according to a 1:1 ratio to receive either carboplatin and paclitaxel or carboplatin and S-1. After a check of patient eligibility, random assignment was performed centrally at the West Japan Oncology Group data center by minimization with stratification factors including disease stage (IIIB *v* IV), type of histology (adenocarcinoma *v* nonadenocarcinoma), sex (male *v* female), and investigator center. The intent-to-treat (ITT) patient population included all patients who underwent random assignment. The per-protocol (PP) population was defined as the ITT population minus patients considered to have major violations of inclusion or exclusion criteria and those who did not receive any protocol treatment. The safety population was defined as all patients receiving at least one dose of study drugs. The primary end point of the study was OS, which was analyzed in the ITT population by estimation of the hazard ratio (HR) and two-sided 95% CI derived from a Cox regression model with adjustment for the stratification factors with the exception of investigator center. Median OS in both treatment arms was assumed to be 14 months on the basis of data from previous clinical trials.[11] Noninferiority of carboplatin and S-1 was to be concluded if the upper limit of the 95% CI of the HR was lower than 1.33; that is, the null hypothesis that the median OS of the carboplatin and S-1 group would be up to 3.48 months shorter than that of the carboplatin and paclitaxel group was analyzed. Demonstration of noninferiority with a statistical power of 85% at a two-sided significance level of .05 and 2 years of follow-up after 2.5 years of accrual would require 263 patients in each treatment group. Given the possibility of variance inflation due to censoring, the sample size was set at 560 (280 per arm). One interim analysis was planned when all the patients had been enrolled. For analysis of the primary end point, adjustment for multiple comparisons was handled by the method of Lan and DeMets, with the use of the O'Brien-Fleming type $\alpha$ spending function. The significance level was set at .008 for the interim analysis, taking the numbers of observed events (n = 268) and expected events (n = 442) into account. Survival curves (PFS and OS) were analyzed by the Kaplan-Meier method and were compared between groups by the Cox regression model. The 95% CI for median PFS and OS was calculated by the method of Brookmeyer and Crowley. Planned subgroup analyses for OS were performed to examine the interaction effect of treatment arm with each of performance status, sex, disease stage, type of histology, and smoking status. Patient characteristics (ie, sex, ECOG PS, histology, clinical stage, and smoking status) as well as response and toxicity incidence were compared between the two treatment arms by the $\chi^2$ test, and age was compared by the Wilcoxon test. Longitudinal QOL data were analyzed with a linear mixed-effects model. All *P* values were two sided. Statistical analyses were performed with SAS for Windows, release 9.1 (SAS Institute, Cary, NC).

## RESULTS

### Patient Characteristics

From August 2006 to May 2008, 564 patients from 30 institutions were enrolled in the study. One patient was excluded from the carboplatin and paclitaxel arm because of loss to follow-up. The ITT population thus consisted of 563 patients: 281 individuals randomly assigned to the carboplatin and paclitaxel group and 282 individuals randomly assigned to the carboplatin and S-1 group (Fig 1). The baseline demographic and disease-related characteristics of the study subjects were well-balanced between the two treatment arms (Table 1). Two patients in the carboplatin and paclitaxel arm and three patients in the carboplatin and S-1 arm did not receive any chemotherapy, with the result that 558 patients were eligible for safety analysis (Fig 1).

### Delivered Chemotherapy

The number of treatment courses administered was 1,037 in the carboplatin and paclitaxel arm (median, 4; range, 1 to 6) and 987 in the carboplatin and S-1 arm (median, 4; range, 1 to 6). Dose reductions occurred in 90 (8.7%) of the carboplatin and paclitaxel courses and in 49 (5.0%) of the carboplatin and S-1 courses. Carboplatin and paclitaxel dose reductions were mainly due to neuropathy, whereas those for carboplatin and S-1 were most commonly attributable to thrombocytopenia. Dose delays occurred in 47.9% of carboplatin and paclitaxel courses and 68.5% of carboplatin and S-1 courses. Delays due to

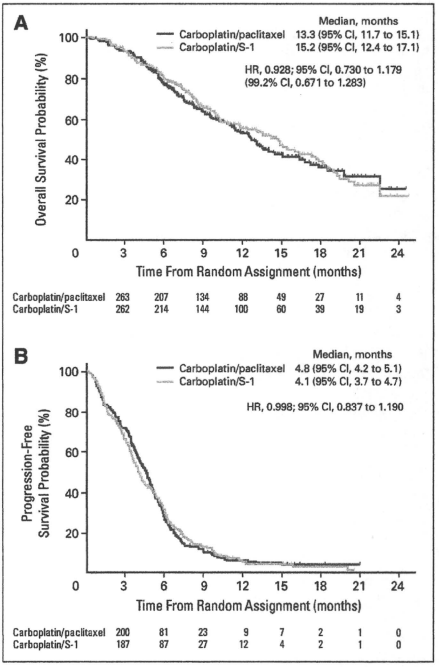


**Fig 2.** (A) Overall survival and (B) progression-free survival for the intent-to-treat population (n = 563). HR, hazard ratio.

  

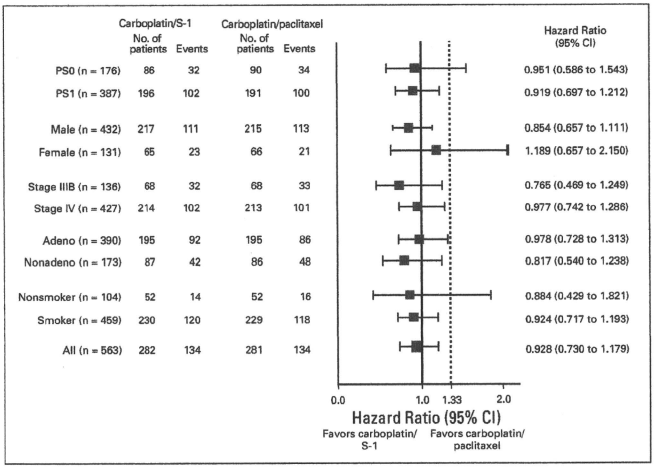


**Fig 3.** Subgroup analysis of overall survival in the intent-to-treat population (n = 563). PS, performance status; Adeno, adenocarcinoma; Nonadeno, nonadenocarcinoma.

hematologic toxicity occurred in a higher proportion of carboplatin and S-1 courses (51.6%) than carboplatin and paclitaxel courses (9.6%). S-1 was administered for the planned 14 days without interruption in 89.1% of carboplatin and S-1 courses. The median relative dose intensities were high for both carboplatin and paclitaxel (89.6% and 87.6%, respectively) and carboplatin and S-1 arms (83.3% and 94.3%, respectively). The most frequent reason for discontinuation of therapy was disease progression in both arms. Treatment was withdrawn before completion from a similar proportion of patients in each group (13.6% for carboplatin and paclitaxel and 10.7% for carboplatin and S-1) because of adverse events.

### *Efficacy*

At the interim analysis planned for when patient enrollment was completed, 268 death events were available in total. The study passed the O'Brien-Fleming boundary of 0.0080 for a positive result with a $P$ value of .002. The HR for OS (carboplatin and S-1 *v* carboplatin and paclitaxel) in the ITT population was 0.928, with a two-sided 99.2% CI after adjustment for multiplicity due to interim analysis of 0.671 to 1.283 (Fig 2A). Noninferiority of carboplatin and S-1 therapy was thus confirmed at the interim analysis by the upper limit of the CI being less than the protocol-specified margin of 1.33. The crude (unadjusted) 95% CI of the HR for OS of 0.928 was 0.730 to 1.179 in the ITT population, and an HR for OS of 0.931 (95% CI, 0.732 to 1.186) was obtained with the PP population. Median OS was 15.2 months (95% CI, 12.4 to 17.1) in the carboplatin and S-1 arm and 13.3 months (95% CI, 11.7 to 15.1) in the carboplatin and paclitaxel arm, with the 1-year survival rates being 57.3% and 55.5%, respectively. Subgroup analysis of OS in the ITT population according to stratification variables and other baseline characteristics were consistent with the primary analysis. A significant interaction effect between treatment arm and subgroups was not observed. The 95% CI for the HR in each subgroup included 1.00 (Fig 3).

The median PFS was 4.1 months in the carboplatin and S-1 arm and 4.8 months in the carboplatin and paclitaxel arm in the ITT population, with a corresponding HR of 0.998 and 95% CI of 0.837 to 1.190 (Fig 2B). In the PP population, the median values of PFS were 4.2 and 4.8 months for the carboplatin and S-1 and carboplatin and paclitaxel arms, respectively, with a corresponding HR of 0.992 and 95% CI of 0.832 to 1.184. Response to treatment was assessed in 279 patients (99.3%) of the carboplatin and paclitaxel group and in 279 patients (98.9%) of the carboplatin and S-1 group. For overall response (CR + PR) rate, carboplatin and paclitaxel was superior to carboplatin and S-1 (29.0% *v* 20.4%; $P = .019$, $\chi^2$ test), whereas the overall disease control (CR + PR + stable disease) rate was similar in both treatment groups (73.5% *v* 71.7%, respectively; $P = .635$).

### *Safety*

The incidence of leukopenia or neutropenia of grade 3 or 4 was significantly lower for patients in the carboplatin and S-1 arm than for those in the carboplatin and paclitaxel arm (leukopenia, 5% *v* 33%; neutropenia, 21% *v* 77%, respectively), as was the incidence of febrile neutropenia (1% *v* 7%; Table 2). Conversely, treatment with carboplatin and S-1 was associated with a higher rate of thrombocytopenia of grade 3 or 4 than was that with carboplatin and paclitaxel (33% *v* 9%, respectively). Platelet transfusion was also necessary for more patients in the carboplatin and S-1 arm than in the carboplatin and paclitaxel arm (8% *v* 2%, respectively; $P = .002$). The overall rates of neuropathy and alopecia were much lower in the carboplatin and S-1 arm (neuropathy, 16% *v* 81%; alopecia, 9% *v* 77%), whereas nausea, vomiting, and diarrhea occurred more frequently in the carboplatin/S-1 arm (Table 2). Death as a result of toxicity occurred in two patients; one death in the carboplatin and S-1 arm was associated with gastrointestinal hemorrhage, and another patient in the carboplatin and paclitaxel arm died of febrile neutropenia and pneumonia.

**Table 2.** Incidence of Drug-Related Toxicities in Randomly Assigned and Treated Patients

| Toxicity | Regimen by Grade (%) | | | | | | *P* | |
|---|---|---|---|---|---|---|---|---|
| | Carboplatin/Paclitaxel (n = 279) | | | Carboplatin/S-1 (n = 279) | | | | |
| | All | 3 | 4 | All | 3 | 4 | All | 3 or 4 |
| Hematologic | | | | | | | | |
| Leukopenia | 86.0 | 29.7 | 2.9 | 55.4 | 5.0 | 0.4 | < .001 | < .001 |
| Neutropenia | 89.6 | 31.9 | 44.8 | 58.3 | 18.3 | 2.9 | < .001 | < .001 |
| Anemia | 82.4 | 14.3 | 2.5 | 86.7 | 15.5 | 3.6 | .165 | .680 |
| Thrombocytopenia | 63.1 | 7.2 | 2.2 | 87.4 | 19.4 | 13.3 | < .001 | < .001 |
| Nonhematologic | | | | | | | | |
| Febrile neutropenia | 7.2 | 6.8 | 0.4 | 1.1 | 1.1 | 0 | < .001 | < .001 |
| Nausea | 49.1 | 2.2 | 0 | 62.4 | 1.8 | 0 | .002 | .475 |
| Vomiting | 23.7 | 1.1 | 0 | 34.1 | 1.8 | 0 | .007 | .837 |
| Diarrhea | 20.8 | 1.1 | 0 | 32.6 | 3.2 | 0 | .002 | .302 |
| Neuropathy: sensory | 81.0 | 2.9 | 0 | 15.8 | 0.4 | 0 | < .001 | .668 |
| Arthralgia | 67.4 | 2.5 | 0 | 7.9 | 0 | 0 | < .001 | .357 |
| Alopecia | 76.7 | | | 9.3 | | | < .001 | |

NOTE. Differences between the two arms were evaluated by the $\chi^2$ test.

### QOL

At random assignment, 99.6% of patients (562 of 564) completed baseline questionnaires, with the questionnaire completion rates being 93.4% at 6 weeks and 90.1% at 9 weeks. Compliance rates were not significantly different between the treatment arms. QOL data were missing in 38 surveys due to death or severe impairment of the patient's general condition, which accounted for 2.3% of the total number of the surveys scheduled. There was no significant difference in the lung cancer subscale of FACT-L between the treatment arms (Fig 4). Scores on the neurotoxicity subscale of FACT/GOG-Ntx had decreased significantly in the carboplatin and paclitaxel arm after two cycles of chemotherapy (Fig 4); the adjusted mean scores at 6 and 9 weeks were 41.2 and 41.0 for the carboplatin and S-1 arm and 38.2 and 37.1 for the carboplatin and paclitaxel arm. The alopecia score was also significantly worse in the carboplatin and paclitaxel arm than in the carboplatin and S-1 arm ($P < .001$, analysis of variance), with the adjusted means at 6 and 9 weeks being 3.8 and 3.7 for carboplatin and S-1 and 1.7 and 1.9 for carboplatin and paclitaxel ($P < .001$ at both 6 and 9 weeks, Tukey-Kramer multiple-comparison test).

### Poststudy Treatment

There were no major differences in poststudy treatment between the two arms. Overall, 69.4% of carboplatin and paclitaxel patients and 75.5% of carboplatin and S-1 patients received an additional line of therapy ($P = .103$, $\chi^2$ test). Docetaxel was administered in 43.4% and 52.0% of patients and epidermal growth factor receptor tyrosine kinase inhibitors were administrated in 24.0% and 27.2% of patients in the carboplatin and paclitaxel and carboplatin and S-1 arms, respectively.

## DISCUSSION

Our phase III study is the first to evaluate the efficacy of an S-1–containing regimen in comparison with standard platinum-doublet chemotherapy for first-line treatment of patients with advanced NSCLC. The primary objective of the study—determination of the noninferiority of carboplatin and S-1 compared with carboplatin and paclitaxel in terms of OS—was met at the planned interim analysis.

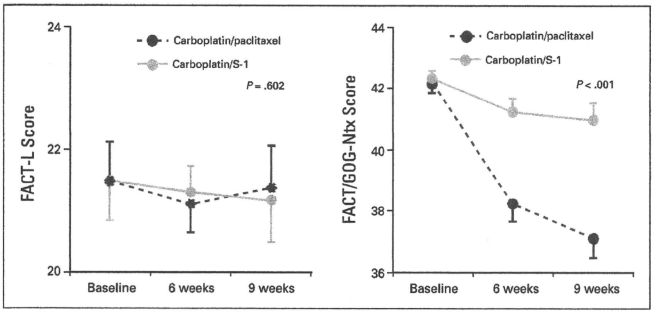


**Fig 4.** Quality of life assessments with the (left) seven-item Functional Assessment of Cancer Therapy–Lung (FACT-L) and (right) 11-item FACT/Gynecology Oncology Group-Neurotoxicity (GOG-Ntx) scales. Data are least square means ± 95% CI. Higher scores indicate better quality of life. *P* values shown were determined by analysis of variance, with *P* being less than .001 for comparison of FACT/GOG-Ntx scores between the two arms at both 6 and 9 weeks by the Tukey-Kramer multiple-comparison test.

  

Analysis of OS in the ITT and PP populations as well as in subgroups of the study subjects demonstrated the noninferiority of carboplatin and S-1. Although there was a significant difference in response rate favoring carboplatin and paclitaxel, disease control rate and PFS were similar for carboplatin and S-1 and carboplatin and paclitaxel. Given that subsequent therapies after discontinuation of the study treatment were well-balanced between the treatment groups, it is unlikely that poststudy therapy confounded survival results. Collectively, our secondary data indicate that the findings of the main analysis are robust. Although the protocol-specified noninferiority margin of 1.33 may be large, the survival curves themselves mostly coincided for the two treatment arms and median OS in the carboplatin and S-1 group was noteworthy at approximately 15 months.

The profile of adverse events associated with carboplatin and S-1 and carboplatin and paclitaxel was as expected, but there were marked differences in the incidence of some of these events. Carboplatin and paclitaxel treatment resulted in a typically high incidence of neutropenia of grade 3 or 4 (76.7%) as well as of febrile neutropenia (7.2%), compared with incidences of only 21.1% and 1.1%, respectively, for carboplatin and S-1. These rates of neutropenia associated with carboplatin and paclitaxel treatment are consistent with those observed in previous studies of Japanese patients.[11,14] Carboplatin and S-1 treatment showed a significantly higher rate of thrombocytopenia, which was the most frequent reason for dose delays in the carboplatin and S-1 group. However, this condition was considered manageable because it was associated with bleeding of grade 3 in only one patient. With regard to nonhematologic toxicities, neuropathy, arthralgia, and alopecia were much less frequent in patients treated with carboplatin and S-1 than in those receiving carboplatin and paclitaxel. Consistent with these results, carboplatin and S-1 treatment showed a clinically relevant improvement in QOL as assessed by the FACT/GOG-Ntx scale and alopecia score. Despite these QOL benefits with carboplatin and S-1, however, there was no significant difference in FACT-L score between carboplatin and S-1 and carboplatin and paclitaxel, possibly because of other more toxic effects of carboplatin and S-1. The incidence of nausea, vomiting, and diarrhea of any grade was higher in patients assigned to the carboplatin and S-1 arm than in those assigned to carboplatin and paclitaxel, although grades 3 or 4 of these toxicities were uncommon (< 4%) in both groups. The relative dose intensity of S-1 was 94.3% in the carboplatin and S-1 arm (median of four cycles administered), and treatment was discontinued in only approximately 10% of patients in this arm because of adverse events. Overall, these data indicate that carboplatin and S-1 was well-tolerated, with continuation of treatment as specified in the protocol not being a problem. According to our previous phase I/II study of carboplatin and S-1,[9] this study excluded elderly (≥ 75 years old) patients. Given its efficacy and favorable toxicity profile, the combination of S-1 and carboplatin warrants further evaluation in elderly patients.

In conclusion, our present study demonstrates the noninferiority of carboplatin and S-1 relative to carboplatin and paclitaxel in terms of OS for patients with advanced NSCLC. Carboplatin and S-1 is therefore a valid therapeutic option for the first-line treatment of patients with advanced NSCLC.

## AUTHORS' DISCLOSURES OF POTENTIAL CONFLICTS OF INTEREST

*Although all authors completed the disclosure declaration, the following author(s) indicated a financial or other interest that is relevant to the subject matter under consideration in this article. Certain relationships marked with a "U" are those for which no compensation was received; those relationships marked with a "C" were compensated. For a detailed description of the disclosure categories, or for more information about ASCO's conflict of interest policy, please refer to the Author Disclosure Declaration and the Disclosures of Potential Conflicts of Interest section in Information for Contributors.*

**Employment or Leadership Position:** None **Consultant or Advisory Role:** Takayasu Kurata, Takeda Pharmaceutical (U) **Stock Ownership:** None **Honoraria:** Isamu Okamoto, Chugai Pharmaceutical, Eli Lilly; Miyako Satouchi, Chugai Pharmaceutical, AstraZeneca; Takayasu Kurata, AstraZeneca, Eli Lilly; Masahiro Fukuoka, AstraZenaca, Daiichi Sankyo, Boehringer Ingelheim, Chugai Pharmceutical; Kazuhiko Nakagawa, Taiho Pharmaciutical, Bristol-Myers Squibb **Research Funding:** None **Expert Testimony:** None **Other Remuneration:** None

## AUTHOR CONTRIBUTIONS

**Conception and design:** Isamu Okamoto, Satoshi Morita, Masahiko Ando, Koji Takeda, Takashi Seto, Nobuyuki Yamamoto, Hideo Saka, Tomonori Hirashima, Miyako Satouchi, Toshiyuki Sawa, Masahiro Fukuoka, Kazuhiko Nakagawa

**Administrative support:** Kenji Tamura, Takayasu Kurata, Masahiro Fukuoka, Kazuhiko Nakagawa

**Provision of study materials or patients:** Isamu Okamoto, Hiroshige Yoshioka, Koji Takeda, Takashi Seto, Nobuyuki Yamamoto, Hideo Saka, Kazuhiro Asami, Tomonori Hirashima, Shinzoh Kudoh, Miyako Satouchi, Norihiko Ikeda, Yasuo Iwamoto, Toshiyuki Sawa, Masaki Miyazaki, Kenji Tamura

**Collection and assembly of data:** Isamu Okamoto, Hiroshige Yoshioka, Satoshi Morita, Masahiko Ando, Koji Takeda, Takashi Seto, Nobuyuki Yamamoto, Hideo Saka, Kazuhiro Asami, Tomonori Hirashima, Miyako Satouchi, Norihiko Ikeda, Yasuo Iwamoto, Toshiyuki Sawa, Masaki Miyazaki, Kenji Tamura, Takayasu Kurata

**Data analysis and interpretation:** Isamu Okamoto, Hiroshige Yoshioka, Satoshi Morita, Masahiko Ando, Nobuyuki Yamamoto, Kenji Tamura, Kazuhiko Nakagawa

**Manuscript writing:** All authors

**Final approval of manuscript:** All authors

## REFERENCES


1. Jemal A, Siegel R, Ward E, et al: Cancer statistics, 2009. CA Cancer J Clin 59:225-249, 2009
2. Azzoli CG, Baker S Jr, Temin S, et al: American Society of Clinical Oncology Clinical Practice Guideline update on chemotherapy for stage IV non-small-cell lung cancer. J Clin Oncol 27:6251-6266, 2009
3. Sandler A, Gray R, Perry MC, et al: Paclitaxel-carboplatin alone or with bevacizumab for non-small-cell lung cancer. N Engl J Med 355:2542-2550, 2006
4. Scagliotti GV, Parikh P, von Pawel J, et al: Phase III study comparing cisplatin plus gemcitabine with cisplatin plus pemetrexed in chemotherapy-naive patients with advanced-stage non-small-cell lung cancer. J Clin Oncol 26:3543-3551, 2008
5. Reck M, von Pawel J, Zatloukal P, et al: Phase III trial of cisplatin plus gemcitabine with either placebo or bevacizumab as first-line therapy for nonsquamous non-small-cell lung cancer: AVAil. J Clin Oncol 27:1227-1234, 2009
6. Shirasaka T, Nakano K, Takechi T, et al: Antitumor activity of 1 M tegafur-0.4 M 5-chloro-2,4-dihydroxypyridine-1 M potassium oxonate (S-1) against human colon carcinoma orthotopically implanted into nude rats. Cancer Res 56:2602-2606, 1996
7. Okamoto I, Fukuoka M: S-1: A new oral fluoropyrimidine in the treatment of patients with advanced non-small-cell lung cancer. Clin Lung Cancer 10:290-294, 2009
8. Kawahara M, Furuse K, Segawa Y, et al: Phase II study of S-1, a novel oral fluorouracil, in advanced non-small-cell lung cancer. Br J Cancer 85:939-943, 2001




 

**9.** Tamura K, Okamoto I, Ozaki T, et al: Phase I/II study of S-1 plus carboplatin in patients with advanced non-small cell lung cancer. Eur J Cancer 45:2132-2137, 2009

**10.** Therasse P, Arbuck SG, Eisenhauer EA, et al: New guidelines to evaluate the response to treatment in solid tumors: European Organisation for Research and Treatment of Cancer, National Cancer Institute of the United States, National Cancer Institute of Canada. J Natl Cancer Inst 92:205-216, 2000

**11.** Ohe Y, Ohashi Y, Kubota K, et al: Randomized phase III study of cisplatin plus irinotecan versus carboplatin plus paclitaxel, cisplatin plus gemcitabine, and cisplatin plus vinorelbine for advanced non-small-cell lung cancer: Four-arm cooperative study in Japan. Ann Oncol 18:317-323, 2007

**12.** Cella DF, Bonomi AE, Lloyd SR, et al: Reliability and validity of the Functional Assessment of Cancer Therapy-Lung (FACT-L) quality of life instrument. Lung Cancer 12:199-220, 1995

**13.** Cella D, Peterman A, Hudgens S, et al: Measuring the side effects of taxane therapy in oncology: The functional assessment of cancer therapy-taxane (FACT-taxane). Cancer 98:822-831, 2003

**14.** Kubota K, Kawahara M, Ogawara M, et al: Vinorelbine plus gemcitabine followed by docetaxel versus carboplatin plus paclitaxel in patients with advanced non-small-cell lung cancer: A randomised, open-label, phase III study. Lancet Oncol 9:1135-1142, 2008



  

Oncogene (2011) 1–10

www.nature.com/onc

ORIGINAL ARTICLE

# Roles of BIM induction and survivin downregulation in lapatinib-induced apoptosis in breast cancer cells with *HER2* amplification

J Tanizaki[1], I Okamoto[1], S Fumita[1], W Okamoto[1], K Nishio[2] and K Nakagawa[1]

[1]*Department of Medical Oncology, Kinki University Faculty of Medicine, 377-2 Ohno-higashi, Osaka-Sayama, Osaka, Japan and* [2]*Department of Genome Biology, Kinki University Faculty of Medicine, 377-2 Ohno-higashi, Osaka-Sayama, Osaka, Japan*

**Lapatinib, a dual tyrosine kinase inhibitor of the epidermal growth factor receptor and human epidermal growth factor receptor 2 (HER2), is clinically active in patients with breast cancer positive for *HER2* amplification. The mechanism of this anti-tumor action has remained unclear, however. We have now investigated the effects of lapatinib in *HER2* amplification-positive breast cancer cells with or without an activating *PIK3CA* mutation. Lapatinib induced apoptosis in association with upregulation of the pro-apoptotic protein BIM through inhibition of the MEK-ERK signaling pathway in breast cancer cells with *HER2* amplification. RNA interference (RNAi)-mediated depletion of BIM inhibited lapatinib-induced apoptosis, implicating BIM induction in this process. The pro-apoptotic effect of lapatinib was less pronounced in cells with a *PIK3CA* mutation than in those without one. Lapatinib failed to inhibit AKT phosphorylation in *PIK3CA* mutant cells, likely because of hyperactivation of the phosphatidylinositol 3-kinase (PI3K) signaling pathway by the mutation. Depletion of PIK3CA (a catalytic subunit of PI3K) revealed that survivin expression is regulated by the PI3K pathway in these cells, suggesting that insufficient inhibition of PI3K-survivin signaling is responsible for the limited pro-apoptotic effect of lapatinib in *HER2* amplification-positive cells with a *PIK3CA* mutation. Consistent with this notion, depletion of survivin by RNAi or treatment with a PI3K inhibitor markedly increased the level of apoptosis in *PIK3CA* mutant cells treated with lapatinib. Our results thus suggest that inhibition of both PI3K-survivin and MEK-ERK-BIM pathways is required for effective induction of apoptosis in breast cancer cells with *HER2* amplification.**

*Oncogene* (2011) **0**, 000–000. doi:10.1038/onc.2011.111

**Keywords:** BIM; survivin; *HER2* amplification; *PIK3-CA* mutation; apoptosis; breast cancer

Correspondence: Dr I Okamoto, Department of Medical Oncology, Kinki University Faculty of Medicine, 377-2 Ohno-higashi, Osaka-Sayama, Osaka, Japan.
E-mail: chi-okamoto@dotd.med.kindai.ac.jp
Received 3 October 2010; revised 17 February 2011; accepted 1 March 2011

## Introduction

Breast cancer is the leading cause of cancer death among women worldwide. Amplification of the human epidermal growth factor receptor 2 (*HER2*) gene occurs in 25–30% of breast cancers (Slamon *et al.*, 1987, 1989), and HER2 is thus an attractive target for the development of therapeutic drugs. Lapatinib, a dual tyrosine kinase inhibitor of HER2 and the epidermal growth factor receptor (EGFR), has shown anti-tumor activity for breast cancer with *HER2* amplification in pre-clinical and clinical studies (Geyer *et al.*, 2006; Konecny *et al.*, 2006; Gomez *et al.*, 2008). Although lapatinib improved the overall outcome for such patients, not all patients were benefited from the treatment. Characterization of the molecular basis of the response to lapatinib will thus be important to maximize the clinical efficacy of this drug.

Mutations in *PIK3CA*, which encodes the p110α catalytic subunit of phosphatidylinositol 3-kinase (PI3K), have been identified in 8–40% of breast cancers (Samuels *et al.*, 2004; Saal *et al.*, 2005; Berns *et al.*, 2007). Although a positive correlation between HER2 overexpression and the presence of *PIK3CA* mutations has been described (Saal *et al.*, 2005), the relation between the efficacy of lapatinib and such mutations has remained unclear (Eichhorn *et al.*, 2008; Toi *et al.*, 2009; Kataoka *et al.*, 2010). We have therefore now investigated the effects of lapatinib in *HER2* amplification-positive breast cancer cells with or without an activating *PIK3CA* mutation, and we further examined the mechanism responsible for the induction of apoptosis in these cells.

## Results

### *Lapatinib inhibits cell proliferation and induces apoptosis in breast cancer cells with* HER2 *amplification*

We first examined the effect of lapatinib on the proliferation *in vitro* of breast cancer cells positive or negative for *HER2* amplification (Figure 1a). All six cell lines with *HER2* amplification, including SK-BR3, ZR-75-30, BT-474, MB-361, MB-453 and HCC1954, were sensitive to lapatinib, with median inhibitory concentration ($IC_{50}$) values ranging from 0.05 to 0.80 μM, which are within the clinically achievable concentration range

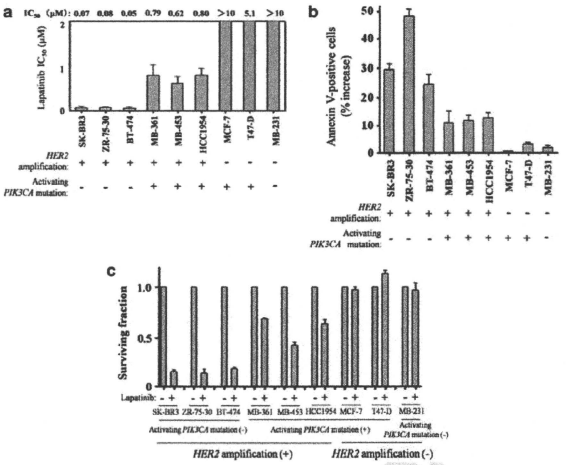


**Figure 1** Effects of lapatinib on cell proliferation and apoptosis in breast cancer cells classified according to *HER2* and *PIK3CA* status. (**a**) The indicated cell lines were cultured for 72 h in complete culture medium containing various concentrations of lapatinib, after which the number of viable cells was determined and the $IC_{50}$ value of lapatinib for inhibition of cell proliferation was calculated. (**b**) The indicated cell lines were incubated for 72 h with lapatinib (1 μM), after which the number of apoptotic cells was determined by staining with annexin V and propidium iodide followed by flow cytometry. The percentage increase in the number of apoptotic cells relative to the corresponding value for cells incubated without lapatinib is shown. (**c**) The indicated cell lines were cultured for 14 days in the presence of lapatinib (1 μM) before determination of the number of colonies for calculation of the surviving fraction relative to that of control cells incubated without lapatinib. All data are means ± s.e. from three independent experiments.

for this drug (LoRusso *et al.*, 2008; Burris *et al.*, 2009). Among these *HER2* amplification-positive cells, those with an activating *PIK3CA* mutation (MB-361, MB-453 and HCC1954) were less sensitive to lapatinib than were those without such a mutation (SK-BR3, ZR-75-30 and BT-474). Cell lines negative for *HER2* amplification, including MCF-7, T47-D and MB-231, were resistant to lapatinib, with $IC_{50}$ values of $>5.0$ μM.

We next examined the effect of lapatinib on apoptosis in these various breast cancer cell lines (Figure 1b). An annexin V binding assay showed that lapatinib (1 μM) induced apoptosis in all *HER2* amplification-positive cells, but was largely without effect in amplification-negative cells. Consistent with the $IC_{50}$ values for the anti-proliferative effect of the drug, the extent of lapatinib-induced apoptosis was less pronounced in *HER2* amplification-positive cells with an activating *PIK3CA* mutation than in those without such a mutation. We further examined the effect of lapatinib on clonogenic survival of breast cancer cells. Again, lapatinib greatly reduced the clonogenicity of *HER2* amplification-positive cells without a *PIK3CA* mutation, whereas the reduction in the number of clones was less marked for those with a *PIK3CA* mutation (Figure 1c). These data thus revealed that lapatinib exerts anti-proliferative and anti-survival effects in cells positive for *HER2* amplification, but the extent of these effects is smaller for such cells with a *PIK3CA* mutation than for those without this genetic change.

*Differential effect of lapatinib on AKT signaling in* HER2 *amplification-positive breast cancer cells with or without an activating* PIK3CA *mutation*

We examined the effects of lapatinib on the AKT and ERK (extracellular signal-regulated kinase) signaling pathways in breast cancer cell lines (Figure 2a). Immunoblot analysis showed that phosphorylation of both AKT and ERK was markedly inhibited by lapatinib in *HER2* amplification-positive cells without an activating *PIK3CA* mutation. In *HER2* amplification-positive cells harboring a *PIK3CA* mutation, however, lapatinib inhibited the phosphorylation of ERK but had little effect on that of AKT. Lapatinib showed little effect on the phosphorylation of AKT or ERK in *HER2* amplification-negative cells. These data thus revealed that, whereas lapatinib inhibited the phosphorylation of ERK in all *HER2* amplification-positive cells, its effect on that of AKT was dependent on *PIK3CA* mutational status.

*Effects of lapatinib on apoptosis-related proteins in* HER2 *amplification-positive breast cancer cells with or without an activating* PIK3CA *mutation*

Given that lapatinib induced apoptosis in cells with *HER2* amplification, we examined its effects on apoptosis-related proteins in these cells (Figure 2b). Immunoblot analysis revealed that lapatinib upregulated the expression of BIM, a pro-apoptotic member of the Bcl-2